Progress In Electromagnetics Research C, Vol. 49, 97–104, 2014

Compact Dual-Band MIMO Antenna with High Port Isolation for WLAN Applications

Hao Qin* **and Yuan-Fu Liu**

Abstract—A compact dual-band MIMO antenna with high port isolation for WLAN applications is proposed. The proposed antenna is basically composed of two monopoles and designed at 2.4/5.2 GHz. High port isolation is achieved by introducing a T-shaped junction on the top surface of the substrate and etching two slots on the ground. The measured bandwidth of the proposed antenna are 2.34–2.55 GHz and 5.13–5.85 GHz, which are suitable for WLAN applications, and the measured isolation between the two monopoles is higher than 20 dB in both bands. Meanwhile, the envelope correlation coefficient of the antenna at both operating bands is lower than 0.001, which means that the antenna has high diversity gain. Good agreement is achieved between the predicted result and the measured data. The overall size of the proposed antenna is 38 mm × 43 mm × 1.6 mm.

1. INTRODUCTION

The development of next-generation wireless communication systems requires higher data rate and higher channel capacity. Meanwhile, there is a trend toward the miniaturization of handheld devices. These conflicting requirements must be met using low-cost solutions that simultaneously maintain high radiation efficiency. One promising solution is MIMO (multiple-input-multiple-output) technology. In MIMO system, multiple parallel wireless routes are created by placing multiple antennas at transferring and receiving terminals. Higher channel capacity and data rate can be acquired without adding extra power or spectrum [1]. Therefore, since the closely spaced antennas can cause strong mutual coupling, it is very difficult to integrate multiple antennas closely in a size restricted device (for example: handset) while maintaining good isolation between antennas [2]. To reduce mutual coupling, many methods have been presented, including the neutralization line [3], etching slots on the ground [4], DMN (decoupling and matching network) composed of series/shunt reactive elements [5], eigenmode DMN approach [6], electromagnetic band-gap (EBG) structure [7], and defected ground structure(DGS) [8]. Moreover, low correlation and diversity polarization are achieved simultaneously after arranging the two folded monopoles orthogonally [9].

The foregoing decoupling techniques in the literature above, though in a general sense provide excellent decoupling capability, are restricted to single band operation. This apparently contradicts to the evolution of modern communication systems, of which dual-band or multiband operations have become essential. Dual-band MIMO antenna using decoupling network has been proposed [10]. The decoupling network, which consists of reactive elements and microstrip lines, can only perform with a narrow band. Moreover, fabricating such a circuit network will bring in additional complexity of the system. In [11], a dual-band MIMO antenna with high port isolation by using an array of printed capacitively loaded loops (CLLs) on the antenna is proposed. A dual-band polarized bowtie antenna array for MIMO WLAN is presented in [12], and a dual-band MIMO antenna with high isolation is

Received 19 February 2014, Accepted 11 April 2014, Scheduled 17 April 2014

* Corresponding author: Hao Qin (casey.hurry.up@gmail.com).

The authors are with the Research Institute of Electronic Science and Technology, University of Electronic Science and Technology of China, Chengdu 611731, China.

proposed by introducing two transmission lines on the top surface of the substrate and etching two slots on the ground [13]. Though good decoupling effect is achieved, such technologies in [11–13] require a significant amount of space. In this paper, a compact dual-band MIMO antenna with high port isolation is proposed. The designed antenna is basically composed of two monopoles and operates at 2.4/5.2 GHz. To achieve low mutual coupling between the two antenna elements, a T-shaped junction on the top surface of the substrate and two slots on the ground are introduced. High port isolation and impedance matching at both operating bands are acquired. Meanwhile, the antenna is compact in size, simple in structure and easy to fabricate. The proposed antenna is smaller in size than the antenna reported in [11–13].

2. ANTENNA DESIGN AND PARAMETRIC STUDY

The geometry with some detailed dimensions of the proposed MIMO antenna is illustrated in Figure 1. The MIMO antenna consists of two symmetric back-to-back monopoles, of which the first monopole (branch 1) is used to excite two resonant frequencies. Based on the mode design method in [14], a rectangular patch (branch 2) is added to straight strip (branch 1) to shift the mode resonant frequency towards a specific frequency, thus two needed bands can be determined, respectively. The MIMO antenna is printed on the front side of a commercial 1.6-mm FR4 substrate with relative permittivity of 4.4 and loss tangent of 0.02. On the back side of the substrate, the rectangular metal of 38 mm in width and 43 mm in length serves as a ground plane for the portable device. The distance between the two monopoles is 14 mm. In order to suppress the mutual coupling, a T-shaped junction connecting the two monopoles and ground plane, and two slots on the ground are introduced. The proposed antenna structure is designed and analyzed by using the Ansoft High Frequency Structure Simulator (HFSS).

Figure 2(a) shows the simulated results for return loss of the monopoles with different lengths of branch 1 (L_1). As L_1 decreases, both lower and upper bands are shifted towards higher frequencies, because both lower frequency and resonant frequency are determined by branch 1. Figure 2(b) shows the return loss for different lengths of L_2. Branch 2 is designed to shift the resonant frequency generated by branch 1. As L_2 decreases, the resonant frequency is shifted towards a high value with little change of the lower band. Therefore, the widths of the two monopoles are used for impedance matching at both operating bands. Furthermore, L_1, L_2, W_1, W_2 can be used to adjust resonant frequencies for a dual-band antenna operating at 2.4 and 5.2 GHz.

In order to reduce the mutual coupling, a T-shaped junction connecting the two monopoles and the ground, and two slots on the ground plane are introduced. The T-shaped junction acts as a short stub-loaded resonator (SSLR) to generate transmission zeros between the two antennas. From Figure 1,

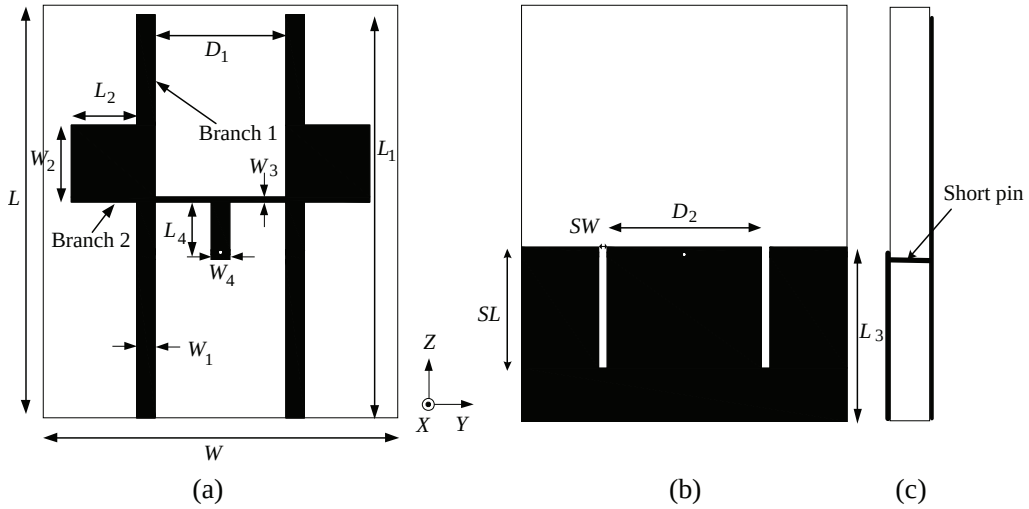

Figure 1. Configuration of the proposed antenna: (a) top view, (b) back view, and (c) side view.

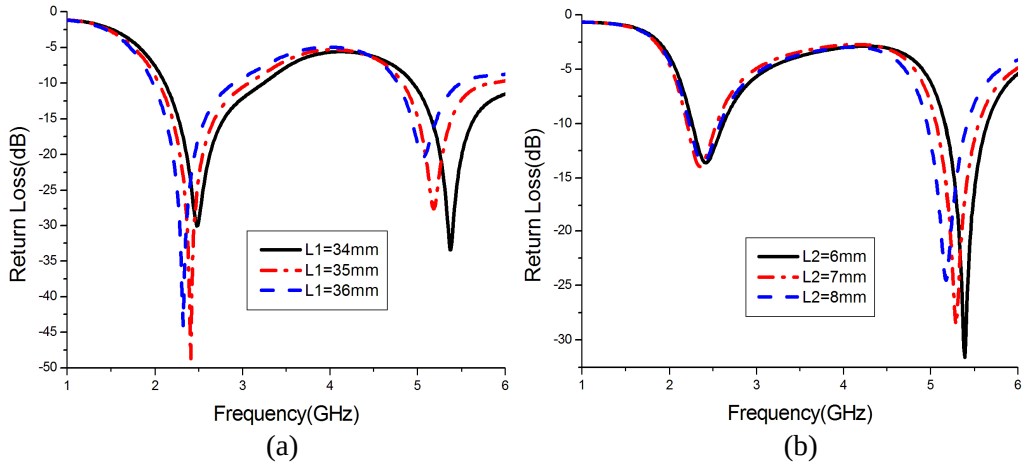

Figure 2. Simulated return loss with varied (a) L_1 and (b) L_2.

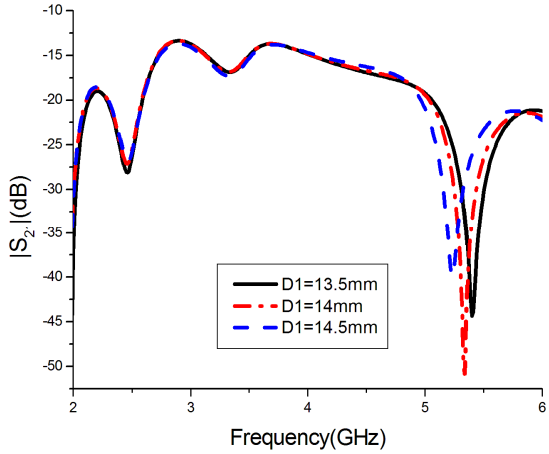

Figure 3. Simulated $|S_{21}|$ with varied D_1.

it can be seen that the T-shaped junction is symmetrical. Therefore, according to [15], the resonant frequencies related to the even and odd T-shaped junction excitation modes are calculated as follows:

$$f_{odd} = \frac{c}{2D_1 \cdot \sqrt{\varepsilon_{eff}}} \tag{1}$$

$$f_{even} = \frac{c}{2\left(D_1 + 2\left(\frac{W_3}{2} + L_4\right)\right) \cdot \sqrt{\varepsilon_{eff}}} \tag{2}$$

$$\varepsilon_{eff} \approx \frac{(\varepsilon_r + 1)}{2} \tag{3}$$

where ε_{eff} denotes the effective dielectric constant of the substrate, and c is the velocity of light in free space. We choose f_{odd} as the upper resonant frequency at 5.2 GHz, while f_{even} is chosen as the lower resonant frequency between 2.4 GHz and 5.2 GHz in order to achieve better decoupling performance. Figure 3 shows the simulated $|S_{21}|$ with different D_1. It is shown that the upper resonant frequency is affected significantly with little change to the lower resonant frequency. Moreover, the change of D_1 has no influence on the resonant frequency at 2.4 GHz since this resonant frequency is generated by two slots on the ground plane. Two slots on the ground plane are used to change the distribution of the ground surface current and act as a $\lambda_g/4$ stub filter operating at 2.4 GHz band to block current toward the other port. The simulated $|S_{21}|$ is studied when the slot lengths (SL) and slot distances (D_2) are

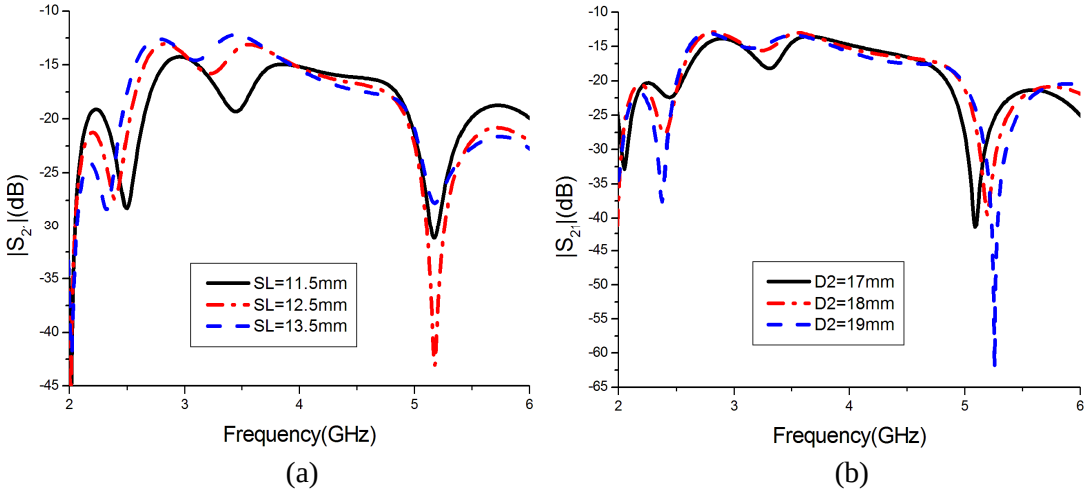

Figure 4. Simulated $|S_{21}|$ for with varied (a) SL and (b) D_2.

Table 1. Parameters of the proposed antenna (see Figure 1).

Parameter	W	L	L_1	W_1	L_2	W_2	L_3	W_3	L_4	W_4	D_1	D_2	SL	SW
Value (mm)	38	43	42	2	7	8	18	0.5	6	2	14	18	12.5	1

varied, as shown in Figure 4. By tuning the length of SL, from Figure 4(a), it is seen that the increase in SL decreases the resonant frequency of the band with no shift in the upper resonant frequency at 5.2 GHz at all. It is also seen that the decoupling effect is achieved when length of the slot is about $\lambda_g/4$ at the operating frequency. From Figure 4(b), all the resonant frequencies are shifted since the slots are moved toward the inner region of the feeding ports. It may be because the strong mutual coupling between slots and the feeding lines affects the proper functioning of the decoupling structure. SL, D_1 and D_2 can be used to adjust isolations at both lower and upper bands. The optimized values for SL, D_1 and D_2 are found to be 12.5 mm, 14 mm and 18 mm for the best isolation at both bands. The optimal values for the antenna dimensions are shown in Table 1.

3. RESULTS AND DISCUSSION

Based on the optimal dimensions listed in Table 1, a prototype of the dual-band MIMO antenna is designed, fabricated, and experimentally investigated. Figure 5(a) shows a photograph of the fabricated antenna. The S-parameters of the dual-band MIMO antenna is measured by the Agilent E8363B vector network analyzer (VNA). For the convenience of comparison, the measured and simulated results of the proposed antenna are plotted in Figure 5(b) and listed in Table 2. Since the two antenna arrays are symmetrically placed, only $|S_{11}|$ and $|S_{21}|$ are given. The measured impedance bandwidths for $|S_{11}| \leq -10$ dB are about 210 MHz (2.34–2.55 GHz) resonated at 2.45 GHz, and 720 MHz (5.13–5.85 GHz) resonated at 5.4 GHz, which can be used for 2.4–2.485 GHz, 5.15–5.35 GHz, and 5.725–

Table 2. Measured and simulated impedance bandwidths of the proposed dual-band MIMO antenna.

	Lower band		Upper band	
	f_1 (GHz)	BW (GHz)	f_2 (GHz)	BW (GHz)
Measured	2.45	2.34–2.55	5.4	5.13–5.85
Simulated	2.41	2.33–2.55	5.2	5.02–5.89

5.825 GHz WLAN bands. As described in Figure 5(b), the measurement result agrees well with the simulation one. Meanwhile, the measured isolation is higher than 20 dB in both lower and upper bands, indicating a good MIMO performance of the structure. The maximum isolation is nearly 33 dB at 2.45 GHz and 44 dB at 5.25 GHz.

The magnitudes of the surface current distributions of the proposed antenna without and with the decoupling structure at 2.4 and 5.2 GHz are illustrated in Figure 6 and Figure 7. From Figure 6(a) and Figure 7(a), we can see that branches 1 and 2 are expected to make the antenna exhibit dual-band characteristic because they present two surface current lengths. Obviously, branch 1 makes the antenna operate at the lower resonant frequency while branch 2 shifts the upper resonant frequency generated by branch 1, and the current distribution is in accordance to the phenomenon in Figure 2. However, there is strong current coupling through the ground current coupling and the near-field coupling since the two antenna arrays are placed closely without decoupling structure. From Figure 6(b) and Figure 7(b), after applying the decoupling structure, the mutual coupling is reduced considerably. In particular, at 2.4 GHz the mutual coupling is strongly prevented by the slots and the T-shaped junction, while at 5.2 GHz its effect is deeply reduced by the presence of the T-shaped junction.

The measured far-field radiation patterns in E-plane (XZ-plane) and H-plane (XY-plane) are given in Figure 8. Radiation patterns are measured in anechoic chamber SATIMO StarLab with one port exited while the other port is terminated with a 50 Ω load, and the peak gain of the proposed antenna is 2.76 dBi at 2.4 GHz and 2.87 dBi at 5.2 GHz.

Envelope correlation coefficient (ECC) is an important parameter to measure the diversity gain of

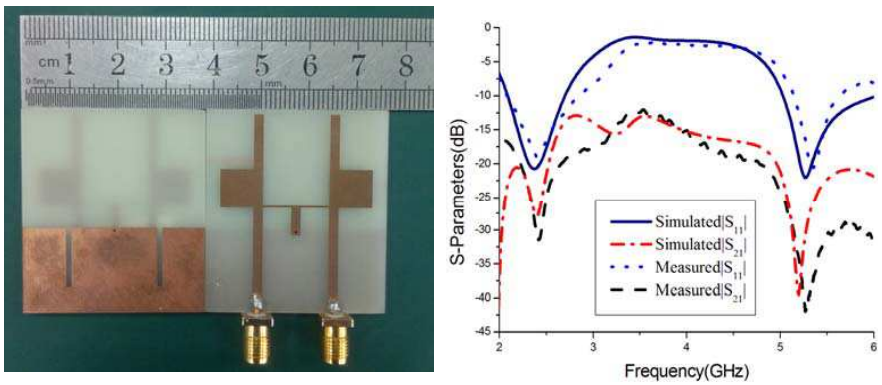

Figure 5. (a) Photograph of the fabricated dual-band MIMO antenna. (b) Measured and simulated S-parameters of the proposed antenna.

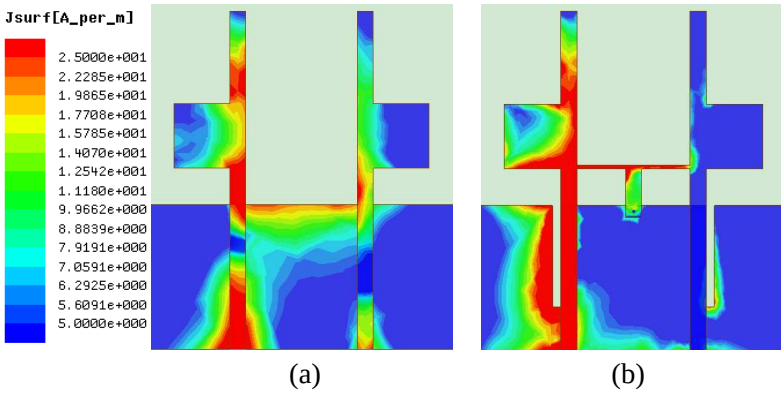

Figure 6. Magnitude of the surface current distribution of the proposed antenna at 2.4 GHz. (a) Without and (b) with decoupling structure.

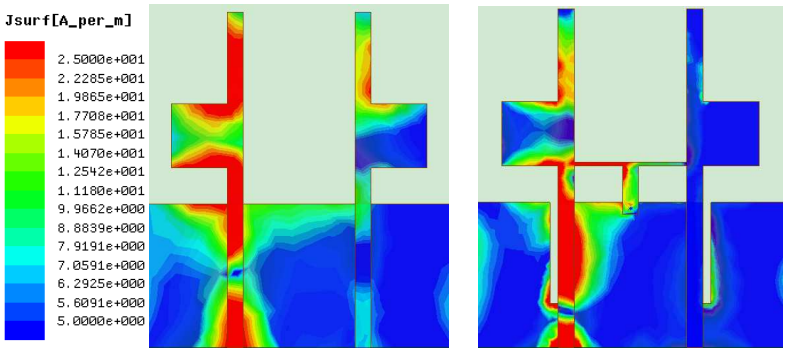

Figure 7. Magnitude of the surface current distribution of the proposed antenna at 5.2 GHz. (a) Without and (b) with decoupling structure.

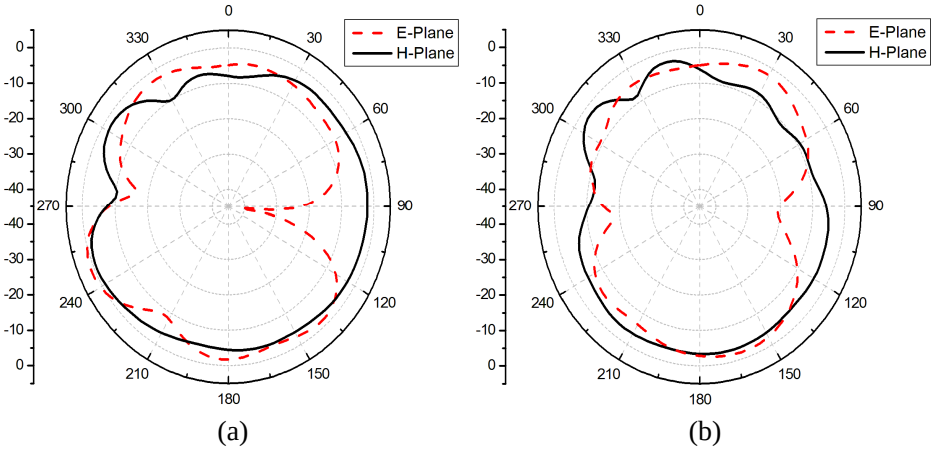

Figure 8. Measured radiation patterns of the proposed antenna at (a) 2.4 GHz, (b) 5.2 GHz.

Table 3. Comparisons of antenna size among proposed antenna and other compact antennas.

Published literature	Antenna purpose	Size comparison (proposed/literature)
Ref. [11]	Dual-band MIMO	32.7%
Ref. [12]	Dual-band MIMO	7.3%
Ref. [13]	Dual-band MIMO	83.8%

a MIMO system. Generally, low envelope correlation always leads to high diversity gain [16]. For a two-antenna system, we can use a simple formula to calculate ECC [17], which is shown in Eq. (4).

$$\mathrm{ECC} = \frac{\left|S_{11}^{*}S_{12} + S_{21}^{*}S_{22}\right|^{2}}{\left[1 - \left(\left|S_{11}\right|^{2} + \left|S_{21}\right|^{2}\right)\right]\left[1 - \left(\left|S_{22}\right|^{2} + \left|S_{12}\right|^{2}\right)\right]} \tag{4}$$

The calculated result for the proposed antenna is given in Figure 9. The desired operating bands of the proposed antenna have an ECC less than 0.001, which means that the antenna has good diversity gain at the operating bands.

Comparisons of the proposed antenna with those presented in [11–13] on antenna dimensions are given in Table 3. Significant reduction in size has been achieved with our antenna design.

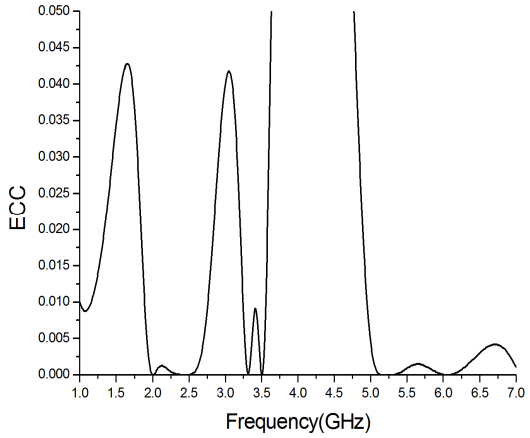

Figure 9. Measured envelope correlation coefficient.

4. CONCLUSION

A compact dual-band MIMO antenna with high port isolation has been presented. The antenna, characterized by a simple structure and compact size of 38 mm × 43 mm × 1.6 mm, satisfies the 10-dB return loss requirement for the WLAN applications with isolations higher than 27 dB at 2.45-GHz band, 40 dB at the 5.2-GHz band and 30 dB at the 5.8-GHz band. The high-isolation performance is achieved by introducing a T-shaped junction on the top of the substrate and etching two slots on the ground. The correlation coefficient of the proposed MIMO antenna is less than 0.001 at both operating bands. In addition, the antenna shows good radiation characteristics and stable gain across the whole working bands. Consequently, the proposed MIMO antenna is suitable for portable wireless devices with a small size.

REFERENCES

1. Jang, Y. U., J. Joung, W. Y. Shin, and E. R. Jeon, "Frame design and throughput evaluation for practical multiuser MIMO OFDMA systems," *IEEE Transactions on Vehicular Technology*, Vol. 60, No. 7, 3127–3141, Jun. 2011.
2. Ozdemir, M. and E. Arvas, "Dynamics of spatial correlation and implications on MIMO systems," *IEEE Commun. Mag.*, Vol. 42, No. 6, S14–S19, 2004.
3. Wang, Y. and Z. W. Du, "A wideband printed dual-antenna system with a novel neutralization line for mobile terminals," *IEEE Antennas and Wireless Propagation Letters*, Vol. 12, 1428–1431, Jun. 2013.
4. Chiu, C. Y., C. H. Cheng, and R. D. Murch, "Reduction of mutual coupling between closely-packed antenna elements," *IEEE Transactions on Antennas and Propagation*, Vol. 55, No. 6, 1732–1738, 2007.
5. Weber, J., C. Volmer, K. Blau, R. Stephan, and M. A. Hein, "Miniaturized antenna arrays using decoupling networks with realistic elements," *IEEE Trans. Microw. Theory Tech.*, Vol. 54, No. 6, 2733–2740, Jun. 2006.
6. Zuo, S.-L., Y.-Z. Yin, Z.-Y. Zhang, W.-J. Wu, and J.-J. Xie, "Eigenmode decoupling for MIMO loop-antenna based on 180° coupler," *Progress In Electromagnetics Research Letters*, Vol. 26, 11–20, 2011.
7. Iluz, Z., R. Shavit, and R. Bauer, "Microstrip antenna phased array with electromagnetic bandgap substrate," *IEEE Transactions on Antennas and Propagation*, Vol. 52, No. 6, 1446–1453, Jun. 2004.
8. Weng, L. H., Y. C. Guo, X. W. Shi, and X. Q. Chen, "An overview on defected ground structure," *Progress In Electromagnetics Research B*, Vol. 7, 173–189, 2008.

9. Park, S. and C. Jung, "Compact MIMO antenna with high isolation performance," *Electron. Lett.*, Vol. 46, No. 6, 154–155, 2010.
10. Karaboikis, M., C. Soras, G. Tsachtsiris, and V. Makios, "Dual-frequency decoupling for two distinct antennas," *IEEE Antennas and Wireless Propagation Letters*, Vol. 11, 1315–1318, Oct. 2013.
11. Sharawi, M. S., A. B. Numan, and D. N. Aloi, "Isolation improvement in a dual-band dual element MIMO antenna system using capacitively loaded loops," *Progress In Electromagnetics Research*, Vol. 134, 247–266, 2013.
12. Zheng, W. C., L. Zhang, Q. X. Li, and Y. Leng, "Dual-band dual-polarized compact bowtie antenna array for anti-interference MIMO WLAN," *IEEE Transactions on Antennas and Propagation*, Vol. 62, No. 1, 237–246, 2014.
13. Cui, S., Y. Liu, W. Jiang, and S. X. Gong, "Compact dual-band monopole antennas with high port isolation," *Electron. Lett.*, Vol. 47, No. 10, 579–580, May 12, 2011.
14. Wong, K.-L. and C.-H. Huang, "Printed loop antenna with a perpendicular feed for penta-band mobile phone application," *IEEE Transactions on Antennas and Propagation*, Vol. 56, No. 7, 2138–2141, 2008.
15. Wang, L., C. Zhao, C. Li, and X. Lin, "Dual-band bandpass filter using stub-loaded resonators with multiple transmission zeros," *2010 9th International Symposium on Antennas Propagation and EM Theory (ISAPE)*, 1208–1211, Guangzhou, China, Nov. 29–Dec. 2, 2010.
16. Vaughan, R. G. and J. B. Anderson, "Antenna diversity in mobile communications," *IEEE Transactions on Vehicular Technology*, Vol. 36, No. 4, 149–171, 1987.
17. Blanch, S., J. Romeu, and I. Corbella, "Exact representation of antenna system diversity performance from input parameter description," *Electron. Lett.*, Vol. 39, No. 9, 705–707, May 2003.